J Solid State Electrochem (1998) 2: 355–361

ORIGINAL PAPER

Lj.D. Arsov · W. Plieth · G. Koßmehl

Electrochemical and Raman spectroscopic study of polyaniline; influence of the potential on the degradation of polyaniline

Received: 12 November 1997 / Accepted: 20 January 1998

Abstract The polymerization of aniline has been studied employing *in-situ* electrochemical and Raman spectroscopical techniques. Aniline was polymerized by cyclic voltammetry on a Pt surface in sulfuric acid solutions of aniline. The Raman bands were assigned for degradation products of the overoxidized form of polyaniline. A discussion of the degradation mechanism is given.

Key words Polyaniline · Electropolymerization · Cyclic voltammetry · Polyaniline degradation · Raman spectroscopy

Introduction

Conducting polymers, especially polyaniline (PANI), were investigated as promising material for the development of organic semiconductors, colour displays, corrosion inhibitors, energy storage devices, rechargeable polymer batteries and opto-electronic devices.

PANI can be prepared chemically or electrochemically by oxidative polymerization. The electrooxidative polymerization method has been preferentially used for the preparation of PANI films, because the deposition of the films can easily be controlled by electrochemical techniques. The morphology of electrochemically prepared PANI depends strongly on the experimental conditions: supporting electrolyte, solvent, current density, potential, nature of electrodes, agitation, temperature etc. The growth rate of a PANI film is apparently dependent on the type of supporting electrolyte in the order: $H_2SO_4 \gg HCl \approx HNO_3 \gg HClO_4$ [1]. This effect is often referred to as "anion effects" [2]. The anion effects are also observed in the electrochemical degradation of PANI film [3]. The rate of polymer overoxidation at relatively high electrode potentials is significantly dependent upon the nature of the anions incorporated in the positively charged polymer [4]. The aniline oxidation reaction is pH dependent in solution of $pH < 2$ in which protonated aniline species react. The oxidation is accompanied by the loss of protons. At higher pH values, non-protonated aniline species participate in the oxidation reaction, which is not pH dependent [5]. The temperature dependence of the polyaniline film voltammetric response in aqueous media has shown that the peak position of the second redox process is affected strongly by the temperature [6]. The film is more stable at low temperatures, probably because of the decrease of the rate of hydrolysis of the quinoid imine structures.

Previous electrochemical studies have shown that, of the electrochemical techniques, cyclic voltammetry (CV) is particularly useful for elucidating basic aspects of the polymer growth and the redox mechanism [7, 8].

In spite of many investigations, there has been a certain controversy regarding the degradation mechanism of PANI [9–11]. So far, few papers have been published dealing with the use of Raman spectroscopy to investigate the dependence of the PANI degradation mechanism on the applied potential [12, 13]. The lack of investigations of the degradation mechanism by Raman spectroscopy is explained by the strong absorption of Raman scattered light from overoxidized PANI. In the overoxidized form of the PANI film, degradation products, which have a weak adhesion and begin to peel off from the electrode surface, are precipitated.

In this paper we describe results of experiments of PANI redox reactions and structure, especially for higher anodic potentials (> 0.26 V vs $Hg/Hg_2SO_4 \cdot 0.5\,M\ H_2SO_4$) (overoxidized PANI). In-situ measure-

Lj.D. Arsov (✉)
Faculty of Technology and Metallurgy, University of St.Cyril and Methodius, 91000 Skopje, Macedonia
Tel.: +389-91-362 031, Fax: +389-91-365 389
e-mail: arsov@ereb.mf.ukim.edu.mk

W. Plieth
Technical University Dresden, Institute of Physical Chemistry and Electrochemistry, Begstr. 66b, D-01062 Dresden

G. Koßmehl
Free University Berlin, Institute of Organic Chemistry, Takustr. 3, D-14195 Berlin-Dahlem

ments are obviously preferable because of questions regarding the integrity of the film after removal from solution; however, very few such studies have been made [14, 15], and none of the overoxidized form and the degradation products. After many (CV) cycles we have succeeded in monitoring Raman bands of degradation products mixed with the oxidized form.

Experimental

Electrodes

The working electrode was made from a 10-mm diameter Pt disc sealed in glass and placed in the spectroelectrochemical cell with a three-electrode configuration. Before each measurement the Pt electrode was polished with different grades of diamond sprays (3, 1 and 0.5 μm). Then, the Pt electrode was cleaned in an ultrasonic bath and rinsed with ethanol. After each measurement the formed film was chemically dissolved in concentrated HNO_3. The counter electrode was a Pt coil with a large surface housed in a separate compartment of the spectroelectrochemical cell. The Hg/Hg_2SO_4 0.5 M H_2SO_4 was used as a reference electrode. All potentials presented in this work refer to this reference electrode.

Spectroelectrochemical cell

The spectroelectrochemical cell was a quartz tube built with three compartments for electrochemical measurements and adopted for simultaneous Raman spectroscopical measurements. The position of the working electrode in a quartz tube could be moved until maximum signal intensity was achieved. The solution in the cell was purged with argon for 15 min prior to the experiments.

Solutions

Aniline (Merck p.a.) was distilled under reduced pressure and kept refrigerated under argon. Sulfuric acid (Merck p.a. 96%) was used as received. Aqueous solutions of 1.0 M H_2SO_4 and 0.1 M $C_6H_5NH_2$ were prepared with deionized and triply distilled water.

The electrochemical equipment consisted of a Model 362 PAR scanning potentiostat and a model 8272 Philips x-2y recorder. The Raman spectra were recorded by a Spex 1877 spectrograph with a silicon photodiode array detector (IRY 512). The measured spectral range was from 580 to 1800 cm^{-1} with a spectral resolution of 3 cm^{-1}. The spectra were excited by the 514.5-nm line of an Ar^+ laser with a power of 100 mW measured on the spectroelectrolytic cell. The measurements were performed in a dark room at an ambient temperature of 20 ± 1 °C.

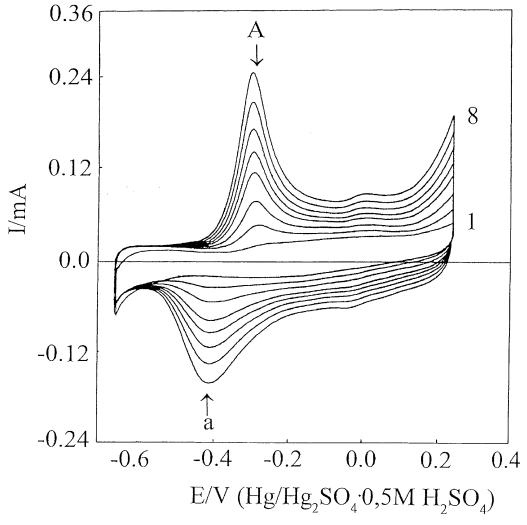

Fig. 1 Cyclic voltammograms on a Pt electrode in aqueous 1.0 M H_2SO_4 + 0.1 M $C_6H_5NH_2$. The number 1 indicates the first cycle of the recorded CV curves. The second, third and fourth curves correspond to the 10th 20th and 30th CV cycle. The fifth sixth and seventh curves correspond to the 35th 40th and 45th CV cycle. The number 8 indicates the 50th CV cycle ($v = 20$ mV/s); potential range −0.65 to +0.25 V

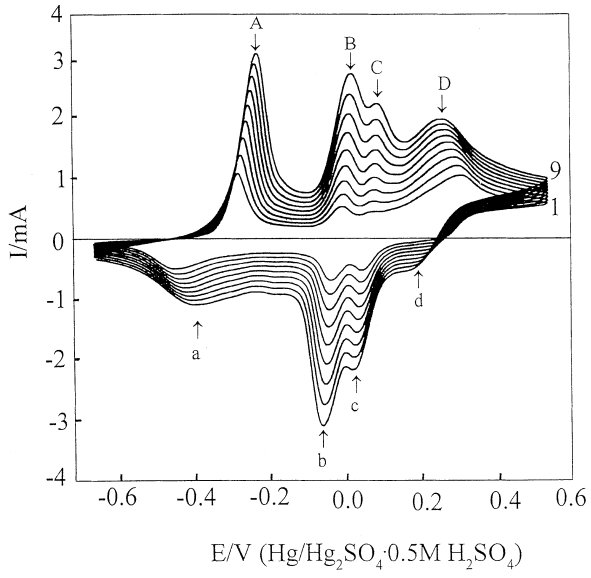

Fig. 2 Cyclic voltammograms on a Pt electrode in aqueous 1.0 M H_2SO_4 + 0.1 M $C_6H_5NH_2$, beginning with the 7th cycle. The numbers 1 and 9 indicate the 7th to the 15th cycle ($v = 20$ mV/s); potential range −0.65 to +0.55 V

Results

In Fig. 1 are presented typical voltammograms recorded on a Pt electrode over the potential range from −0.65 to +0.25 V.

The increasing current indicates the growth of film thickness, and a pair of well-defined redox peaks A/a gradually form. The position of redox peaks does not shift with increasing cycle number, even after 50 cycles, which confirms that these are reversible redox reactions independent of the thickness of the film. A number of authors [16–18] agree that during cyclization transitions between a fully reduced and a fully oxidized film occur (Eq. 1).

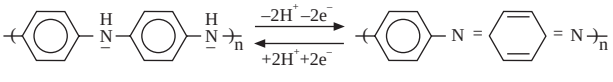

(1)

On continued polarization toward higher anodic potential, up to +0.55 V, on the voltammograms, four pairs of redox peaks are observed (Fig. 2).

The multiple redox peaks indicate the complexity of the redox processes, involving coupled electron transfer

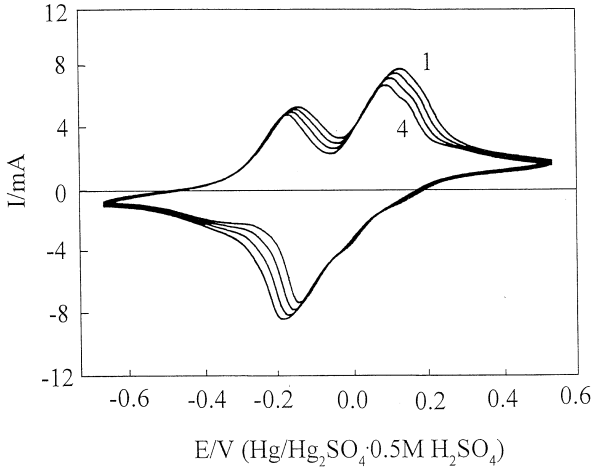

Fig. 3 Cyclic voltammograms on a Pt electrode in aqueous 1.0 M H_2SO_4 + 0.1 M $C_6H_5NH_2$. The numbers 1 and 4 indicate the 26th to the 32nd cycle ($v = 20$ mV/s); each second cycle is recorded potential range is as in Fig. 2

reactions. Peaks D/d only appear after the first 5 cycles.The peaks B/b and C/c gradually grow and become more pronounced. These middle peaks (according to a number of authors [8, 9, 19]) have been attributed to the oxidation and reduction of degradation products. In the earlier stage, polymer growth predominates (peaks A/a).

After the formation of PANI film by successive potential cycling of Pt electrode between −0.65 V and 0.25 V (Fig. 1), the electrode was transferred to 1 M H_2SO_4 and the same procedure of potential cycling as in Fig. 1 was repeated. The Pt electrode showed CV curves similar to those in Fig. 1, but the current did not increase in each succeeding cycle. There was no significant shift in the shape of the recorded curves, even after 100 cycles. The film thickness did not grow because there was no aniline monomer in the supporting electrolyte. On continued polarization toward higher anodic potentials, up to 0.55 V, in the beginning of the voltammograms, four pairs of redox peaks are observed, similar to Fig. 2. Afterwards, the peaks gradually diminished as a result of gradual degradation of the PANI film.

redox reactions increases. This is manifested by shifting of peaks A/a anodically and peaks D/d cathodically. As a result of thicker film formation, the mass transfer (egress of hydronium ions and ingress of anions) limits the electrochemical process. The CVs begin to loose their initial shapes, and after 26 cycles the overoxidized PANI state is obtained; the middle peaks amalgamate with the peak D/d (Fig. 3).

We have performed simultaneously electrochemical and *in-situ* Raman spectroscopic measurements. Potentiostatically controlled Raman measurements have been made for various fixed potentials from the fully reduced form to the fully oxidized form. From the observed differences in the spectra, we expect some information about the change of the PANI structure. The Raman spectra are shown in Fig. 4.

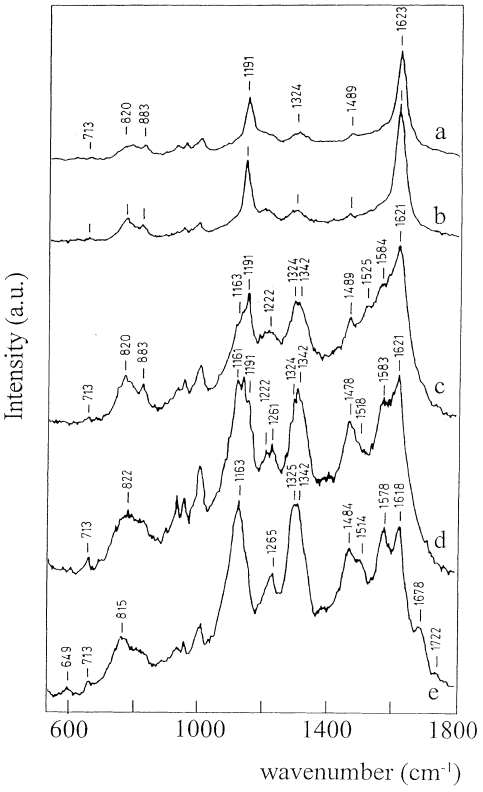

Fig. 4 In-situ Raman spectra measured on a Pt electrode in 1 M H_2SO_4 + 0.1 M $C_6H_5NH_2$ for various fixed potentials after 15 CV cycles between −0.65 and 0.55 V, *a* −0.7 V, 30 min polarization, *b* −0.35 V, 30 min polarization, *c* −0.15 V, 30 min polarization, *d* −0.02 V, 30 min polarization, and *e* 0.2 V immediately after the last cycle

After 15 CV cycles performed in the potential range between −0.65 and +0.55 V (Hg/Hg_2SO_4 0.5 M H_2SO_4) the potential was stopped at −0.7 V (Hg/Hg_2SO_4 0.5 M H_2SO_4), characteristic of the fully reduced PANI form, and after 30 min polarization the Raman spectrum was measured (Fig. 4a). If polarization is shifted more and more to anodic potentials, as can seen in Fig. 4, several bands disappear and several new bands appear. In Table 1 are also listed the Raman bands assigned to the fully reduced PANI form. The most dominant bands are at 1191 cm^{-1} and 1623 cm^{-1}, which are the key bands for *p*-disubstituted benzene rings. This confirms that the fully reduced PANI film is mostly composed of *p*-disubstituted benzene rings.

For lower cathodic potentials at −0.35 V (just before the CV peak A of Fig. 2), the Raman spectrum Fig. 4b shows a similar spectral pattern. The lower intensity of Raman bands at a potential of −0.7 V is probably caused by hydrogen evolution. At potentials negative to the CV peak A the PANI film has the spectra characteristics of the fully reduced form. At −0.15 V (more anodic than the CV peak A of Fig. 2) there is a substantial change (Fig. 4c), i.e. a decrease in intensity of the 1191 cm^{-1} band and the appearance of new bands located at 1163, 1222, 1342, 1525 and 1584 cm^{-1}. These new bands characterize the formation of semiquinone

radical cations, i.e. the *p*-disubstituted benzene rings begin to transform into polarons.

The first redox wave A/a in the CV curves correspond to the removal of electrons from the nitrogen atoms of the amine between the benzene rings. This process leads to a radical cation-like character of the nitrogen atoms [20, 21].

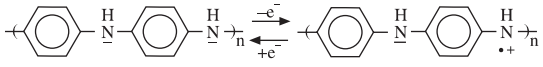

(2)

These transitions occur favourably at higher anodic potentials, ($E > -0.02$ V). Raman bands show that the concentration of semiquinone radical cations in the film has increased (Fig. 4d).

The waves D/d in the cyclic voltammogram (Fig. 2) can be assigned to the oxidation/reduction of the polaron state:

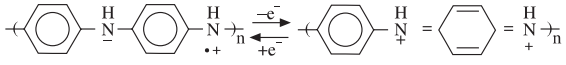

At a potential of $+0.20$ V, bands of a mixture of three oxidation products of PANI are observed: first oxidation step (formation of radical cations), fully oxidized step and overoxidized step with formation of degradation products.

The fully oxidized PANI form is characterized by the transformation of the semiquinone radical cation (polaron) to quinone imine (biradical bication or bipolaron), verified by the Raman bands at 1261, 1478 and 1518 cm^{-1}. The wave numbers of these bands are characteristic of both semiquinone radical cations and quinoid rings; however, in the case of quinoneimine, they are shifted toward higher wave numbers and gain in intensity. The small shift (1261 to 1265 and 1478 to 1484 cm^{-1}) is caused by the low concentration of quinoid rings in the polymer chain. This indicates that the yield of transition radical cation to quinone imine (Eq. 3) is less than 100%.

For potentials more positive than the CV peak D, PANI becomes overoxidized and degradation products occur. The Raman spectrum in Fig. 4e also shows the existence of C=O bonds by the peak at 1678 cm^{-1} and shoulder at 1722 cm^{-1}. We propose the following mechanism:

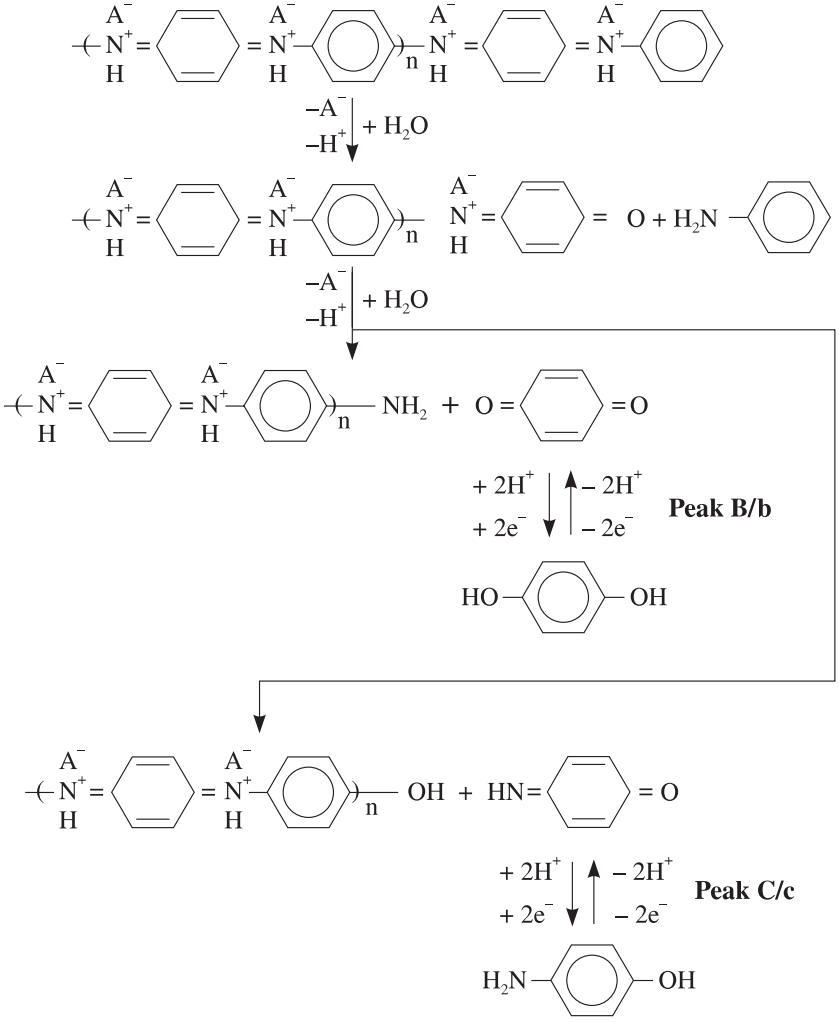

Table 1 Raman frequencies in the 580–1800 cm^{-1} range for various redox forms and degradation products of PANI. B, benzoid ring; Q, quinoid or semiquinoid ring; s, strong; m, middle; w, weak; sh, shoulder; the peaks located at 979, 1005 and 1048 cm^{-1}, which appear in all Raman spectra, belong to the starting solution of 1 M H_2SO_4 + 0.1 M $C_6H_5NH_2$

Potential V/vs Hg/Hg_2SO_4 0.5 M H_2SO_4				Raman assignment	Wilson notation
−0.35	−0.15	−0.02	0.2		
/	/	/	649 w	δ_{C-C} in paradisubstituted B ring	6 b
713 sh	713 sh	713 w	710 w	γ_{C-C} in paradisubstituted B ring	4
820 sh	820 sh	822 sh	815 sh	δ_{C-C} in B ring	1
883 w	883 sh	/	/	γ_{C-H} in B and Q ring	10a
/	1163 s	1161 s	1163 s	δ_{C-H} in Q semiquinone ring	9a
1191 s	1191 w	1191 w	1191 w	δ_{C-H} in B ring	9a
/	1222 w	1224 w	/	ν_{C-N} in B ring	
/	/	1261 m	1265 m	ν_{C-N} in Q ring (semiquinoid end quinoid part)	
1324 sh	1324 sh	1324 m	1325 m	$\nu_{C-N} + \nu_{C-C}$ in B	
/	1342 sh	1342 m	1342 m	(polaronic part)	
1489 w	1489 w	1478 m	1484 m	$\delta_{C=N}$ head to tail polymerization	
/	1525 sh	1518 sh	1514 w	in Q (semiquinoid and quinoid part)	
/	1584 sh	1583 w	1578 m	$\nu_{C=C}$ in B and Q ring (semiquinoid and quinoid part)	8b
1623 s	1621 s	1621 m	1618 m	$\nu_{C=C}$ in B ring	8a
/	/	/	1678 m		
/	/	/	1722 sh	$\nu_{C=O}$ in Q ring	

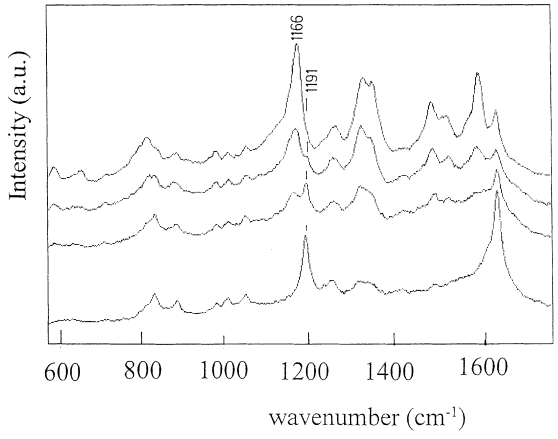

Fig. 5 In-situ Raman spectra on a Pt electrode in aqueous 1.0 M H_2SO_4 + 0.1 M $C_6H_5NH_2$ during the I–E scan from −0.7 to 0.275 V ($v = 50$ mV/min). Spectra are continuously recorded each 2 min. For clarity only the spectra recorded after 2, 12, 14 and 16 min are presented

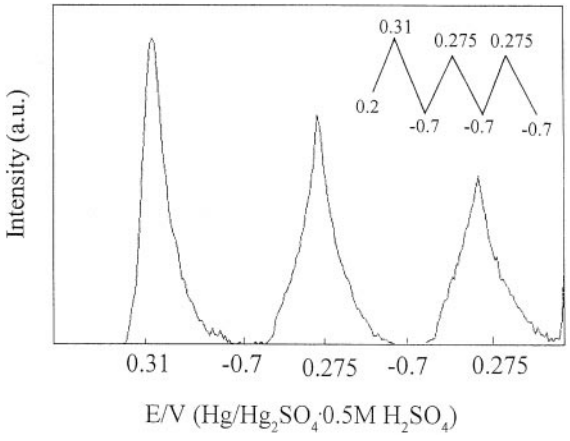

Fig. 6 Raman voltammogram recorded on a Pt electrode in aqueous 1.0 H_2SO_4 + 0.1 M $C_6H_5NH_2$ at a wave number of 1166 cm^{-1} during the I–E scan. The curve is corrected by subtraction of the background ($v = 50$ mV/min)

The final degradation products consist of *p*-benzoquinone, hydroquinone, *p*-aminophenol, quinoneimine, and still-oxidized PANI. As has been already pointed out [9, 10], the *p*-benzoquinone, hydroquinone, *p*-aminophenol and quinoneimine form a dark green precipitate.

The redox waves B/b and C/c of the CV, after about 5 cycles (Fig. 2), come from the oxidation and reduction of *p*-benzoquinone/hydroquinone and *p*-aminophenol/quinoneimine. The products are soluble in aqueous solutions and peel off the electrode surface.

It should be mentioned that with overoxidation the polymer film is not completely destroyed. If the overoxidized film is polarized at a potential of −0.7 V (corresponding to the fully reduced form) and kept for some time at this potential, in the following cycle, the CV curves will have a similar shape to that shown in Fig. 2. This indicates that the redox reactions in the polymer film, (Eqs. 1–3) are independent of the existence of degradation products. This assumption was corroborated by stirring the solution before the cycling. With stirring, the removal of the precipitate of degradation products from the electrode surface is accelerated. After stirring, the CV curves of Fig. 3 change shape, leading to shapes similar to Fig. 2. If the stirring time is increased, the redox peak D/d in the CV curve moves toward higher anodic potentials.

Discussion

All spectroelectrochemical measurements, so far, explain the fact that in acidic electrolyte the polymer can exist in

various oxidation states characterized by the ratio of imine to amine structure [14, 22–24]. Diphenyl-1,4-phenylenediamine was chosen as a model compound for the fully reduced leucoemeraldine base and diphenyl-1,4-phenylenediimine for the fully oxidized pernigrinaline base. The Raman measurements in this paper were carried out with the green laser line because green excitation gives strong bands for both the benzoid and quinoid rings. The blue laser excitation gives strong resonance bands only of the reduced and semioxidized forms. The spectra are bleached by further oxidation. With green laser excitation the bleaching is considerably slower. It was possible to detect the Raman bands of degradation products of overoxidized PANI containing C═O bonds. From electrochemical measurements, Hand and Nelson have proposed the formation of benzoquinone and hydroquinone as degradation products [10]. Later Kobayashi et al. have given a more detailed mechanism of PANI degradation [9]. Recently Yoon-Bo Shim et al. have also included *p*-aminophenol as a degradation product [25]. The strongest Raman band of pure benzoquinone at 1654 cm^{-1}, reported by Quillard et al. [26] and detected with red laser light, is close to the band of this paper at 1678 cm^{-1}. The band is attributed to the C═O bond. The band shift is caused by the mode of the excitation laser. The other band assignments of Quillard et al. [26] for the fully oxidized and the fully reduced PANI form are based on valence-force-field models. Vibrations between CC, CH and CN are included. The bands of degradation products were not taken into account. Bands at lower wave numbers (829 and 649 cm^{-1}, characteristic of *p*-disubstituted benzene rings) are not discussed.

By Raman spectroscopy, the fully oxidized PANI form in the corresponding potential region before and after peak D on the CV curves in Fig. 2 could not be separately detected. Before the CV peak D it is possible only to detect mixtures of emeraldine, pernigrinaline and degradation products. Raman measurements at potentials positive to CV peak D give a broad luminescence background from nonadherent precipitates. At a potential of 0.2 V (Hg/Hg_2SO_4 0.5 M H_2SO_4), cathodic to the CV peak D, the Raman spectra show peaks characteristic of fully oxidized, overoxidized, and degradation products.

CV peak D of the cyclic voltammogram has a strong influence on the efficiency of redox processes. This efficiency decreases with the number of cycles. For example, the small shoulders at 1489 cm^{-1} in Fig. 4a and b indicate that, even in the reduced form of PANI, small amounts of quinoid structure exist. With increasing oxidation, these shoulders grow into separate lines, and the characteristic bands of benzoid rings decrease in intensity.

Figure 5 shows the sequence of change in intensity of two dominant Raman bands during the cyclization from −0.7 V to 0.275 V.

During the successive potential scan from −0.7 V in the anodic direction, the decreasing intensity of Raman bands at 1191 cm^{-1} and increasing intensity of the band at 1166 cm^{-1} are due to the transition of benzoid to quinoid rings. The similar change of the intensity of these two bands with pH was described by M. Bartonek et al. [22]. Higher pH values correspond to more anodic potentials.

Figure 6 shows the Raman cross section of the band at 1166 cm^{-1}.

It is evident that with each new cycle the Raman voltammogram loses intensity. The reason is the degradation of the polymer film.

Conclusion

Electrochemical and simultaneous Raman spectroscopic measurements lead to the following conclusions.

Reversible redox reactions of reduced/semioxidized PANI and the transition between insulator and conducting state are only stable if the anodic potential is limited to less than 0.25 V. For higher potentials, new redox waves occur corresponding to full oxidation and overoxidation of PANI (degradation).

Scanning the potential in the anodic direction, the following transitions in the polymer film are observed: imino-1,4-phenylene → radical cation of imino-1,4-phenylene, (polaron, semiquinone) → nitrilo-2,5-cyclohexadiene-1,4-diylidenenitrilo-1,4-phenylene, (biradical bication or bipolaron). The yield of these transitions is less than 100%. Fully oxidized or overoxidized PANI gives rise to Raman spectra of C═O bands and degradation products: benzoquinone, aminophenol, hydroquinone and quinoneimine.

References

1. Nunziante P, Pistoia G (1989) Electrochim Acta 2: 223
2. Lippe J, Holze R (1992) J Electroanal Chem 339: 411
3. Duic Lj, Mandic Z (1992) J Electroanal Chem 335: 207
4. Kalaji M, Nyholm L, Peter LM (1991) J Electroanal Chem
5. Tang H, Kitani A, Shiotani M (1996) Electrochim Acta 41(9): 1561
6. Inzelt G (1990) J Electroanal Chem 279: 169
7. Stilwell DE, Park SM (1988) J Electrochem Soc 135: 3132
8. Stilwell DE, Park SM (1988) J Electrochem Soc 135: 2491
9. Kobayashi T, Yoneyama H, Tamura H (1984) J Electroanal Chem 177: 293
10. Hand R, Nelson R (1974) J Am Chem Soc 6: 850
11. Zhang AQ, Cui CQ, Lee JY (1995) Synth Met 72: 217
12. Arsov Lj (1998) J Solid State Electrochem (in press)
13. Efremova A, Arsov Lj (1992) J Serb Chem Soc 57 (2): 127
14. Kuzmany H, Sariciftci N (1987) Synth Met 18: 53
15. Bartonek M, Kuzmany H (1991) Synth Met 18: 57
16. Rudzinski WR, Lozano L, Walker M (1990) J Electrochem Soc 137: 3132
17. Genies E, Lapkowski M (1987) J Electroanal Chem 220: 67
18. Hjertberg T, Sandberg M, Wennerstrom O, Lagerstedt I (1987) Synth Met 21: 31
19. Genies E, Lapkowski M, Penneau J (1988) J Electroanal Chem 249: 97

20. Efremova A, Regis A, Arsov Lj (1994) Electrochim Acta 39: 839
21. Stillwell DE, Park SM (1988) J Electrochem Soc 135: 2254
22. Bartonek M, Sariciftci N, Kuzmany H (1990) Synth Met 36: 83
23. Holze R (1987) J Electroanal Chem 224: 253
24. Holze R (1987) Electrochim Acta 32: 1527
25. Shim YB, Won MS, Park SM (1990) J Electrochem Soc 137: 538
26. Quillard S, Louran G, Buisson I, Lefrant S (1993) Synth Met 55–57: 475